Microwave-controlled coupling of Majorana bound states

Thomas L. Schmidt, Andreas Nunnenkamp and Christoph Bruder

Department of Physics, University of Basel, Klingelbergstrasse 82, CH-4056 Basel, Switzerland

E-mail: thomas@thoschmidt.de

Abstract. We propose microwave-controlled rotations for qubits realized as Majorana bound states. To this end we study an inhomogeneous Kitaev chain in a microwave cavity. The chain consists of two topologically nontrivial regions separated by a topologically trivial, gapped region. The Majorana bound states at the interfaces between the left (right) regions and the central region are coupled, and their energies are split by virtual cotunneling processes. The amplitude for these cotunneling processes decreases exponentially in the number of sites of the gapped region, and the decay length diverges as the gap of the topologically trivial region closes. We demonstrate that microwave radiation can exponentially enhance the coupling between the Majorana bound states, both for classical and quantized electric fields. By solving the appropriate Liouville equation numerically we show that microwaves can drive Rabi oscillations in the Majorana sector. Our model emerges as an effective description for a topological semiconducting nanowire in a microwave cavity. Thus, our proposal provides an experimentally feasible way to obtain full single-qubit control necessary for universal quantum computation with Majorana qubits.

1. Introduction

Majorana bound states (MBS) [1] are currently a strong focus of research in the condensed-matter community [2, 3, 4]. Semiconductor nanowires with strong Rashba spin-orbit coupling have emerged as a promising platform to host MBS. Following theoretical proposals [5, 6, 7] first experimental signatures of MBS have recently been reported [8, 9, 10, 11].

On the one hand, MBS are fascinating quantum systems in their own right. On the other hand, MBS could become useful for quantum computing as braiding leads to topologically-protected quantum gates which are immune against certain types of noise [12]. However, these braiding operations do not form a universal set of gates needed for quantum computation, so they have to be supplemented by other gates which are not topologically protected. The circuit quantum-electrodynamics (circuit-QED) architecture [13] offers a controlled and well-developed toolbox in the microwave domain and is thus an ideal candidate to complement the topologically-protected braiding operations. Coupling MBS of a Kitaev chain to a microwave strip-line resonator has recently been studied by Trif and Tserkovnyak [14].

We propose to use microwaves to control the coupling between two MBS which is potentially relevant in the context of quantum computation. In Ref. [15], we investigated the essential features of the proposed coupling scheme in a simplified effective model using perturbation theory in the electron-photon coupling. Here, we confirm and extend those results by numerically solving the Kitaev Hamiltonian in the presence of microwave radiation. The remainder of this paper is organized as follows. In Section 2 we introduce the Hamiltonian for an inhomogeneous Kitaev chain consisting of two topologically nontrivial regions separated by a topologically trivial, gapped region. In this situation it it is well-known that MBS form at the interface between the topologically different regions [1]. We demonstrate that virtual cotunneling processes mediated by the gapped region couple the MBS and split their energies. The amplitude for these processes decreases exponentially in the length of the gapped region, and the decay length diverges as the gap in the topologically trivial region closes. The Kitaev model is known to be an effective description for a topological nanowire [16]. In Section 3 we study its coupling to the microwave field inside a cavity. We find that the cavity field gives rise to a modulation of the hopping matrix element between neighbouring lattice sites. This enables us to control the properties of the chain with the microwave field. In Section 4 we then discuss a Kitaev model coupled to a microwave field. We assume that the cavity field can be described classically before solving the full quantum master equation for a damped, driven as well as quantized photon field. In both cases we find that the microwaves can induce Rabi oscillations in the Majorana sector. They can thus supplement topologically-protected braiding operations to gain full single-qubit control which is a necessary step toward a universal set of quantum gates for Majorana qubits.

2. Inhomogeneous Kitaev chain

To describe a one-dimensional wire which can be brought to either a topologically trivial or topologically nontrivial phase by tuning the system parameters, we shall use the Hamiltonian

of the Kitaev chain [1]. This model captures qualitatively many features of more realistic 1D models [6, 7], while remaining exactly solvable. This makes it very useful for investigating the properties of MBS. In fact, it has been shown that there exists an approximate mapping between realistic models and the Kitaev chain Hamiltonian, so their low-energy degrees of freedom are identical [16]. We shall extend this mapping to incorporate electron-photon coupling in Sec. 3.

We start with a brief review of some essential properties of an *inhomogeneous* Kitaev chain, containing two topologically nontrivial regions, separated by a short topologically trivial, gapped region. On a very general level, this system can be modeled as a Kitaev chain consisting of N sites with position-dependent parameters,

$$H_K = -\sum_{n=1}^{N} \mu_n c_n^\dagger c_n - \frac{1}{2}\sum_{n=1}^{N-1} \left(t_n c_n^\dagger c_{n+1} + \Delta_n c_n c_{n+1} + \text{h.c.} \right). \tag{1}$$

Here, μ_n denotes the onsite energies, t_n are the hopping amplitudes, and Δ_n are the p-wave pairing strengths. The operator c_n ($c_n^\dagger$) annihilates (creates) a spinless fermion at lattice site n. This bilinear Hamiltonian can be diagonalized exactly for arbitrary parameters and will be used below for numerical results. To obtain simple analytical expressions, it is convenient to select the simplest parameter constellation which generates the desired topological phases. We therefore assume Eq. (1) to be of the form

$$H_K = H_L + H_C + H_R + H_{LC} + H_{RC}, \tag{2}$$

where the N-site chain is split into three parts: H_L and H_R describe the left ($n \leq m_1$) and right ($n \geq m_2$) parts of the chain, and H_C the $N_C = m_2 - m_1 - 1$ sites in the central part ($m_1 + 1 \leq n \leq m_2 - 1$). The sections are coupled by H_{LC} that connects sites m_1 and $m_1 + 1$, and H_{RC} that connects sites $m_2 - 1$ and m_2.

The left and right regions are supposed to be in the topologically nontrivial phase, i.e., we assume $\mu_n = 0$ and constant $\Delta_n = t_n =: t > 0$. Then, the Hamiltonians $H_{L,R}$ become diagonal in a basis of nonlocal Dirac fermions, $d_n = \text{Im}\, c_{n+1} + i\text{Re}\, c_n$,

$$H_L = t\sum_{n=1}^{m_1-1} d_n^\dagger d_n, \qquad H_R = t\sum_{n=m_2}^{N-1} d_n^\dagger d_n. \tag{3}$$

In the central part of the chain, we choose the parameters as $\mu_n = \mu_C$, $t_n = t$, and $\Delta_n = 0$. Without loss of generality, we assume $\mu_C > 0$. Since this parameter choice makes the central region topologically trivial, we retain the basis of local Dirac fermions c_n,

$$H_C = -\mu_C \sum_{n=m_1+1}^{m_2-1} c_n^\dagger c_n - \frac{t}{2}\sum_{n=m_1+1}^{m_2-2} \left(c_n^\dagger c_{n+1} + \text{h.c.} \right). \tag{4}$$

To diagonalize H_C, it is convenient to extend the central region to a large number of sites $N_\infty \gg N_C$ and then impose periodic boundary conditions. We shall discuss the quality of this approximation by comparing it to numerical results below. Hence, we introduce the operators $\tilde{c}_n$, where $\tilde{c}_n = \tilde{c}_{n+N_\infty}$. They are defined to coincide with the original operators c_n

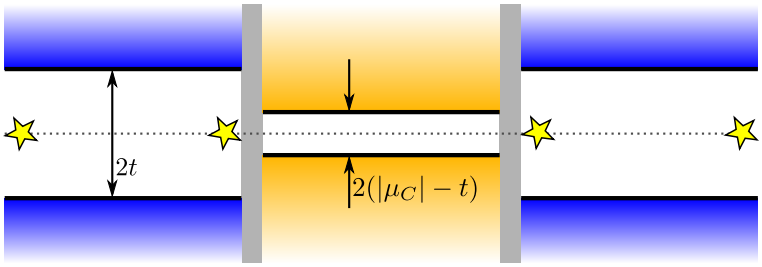

Figure 1. Band structure of the inhomogeneous Kitaev chain in the gapped regime: the left and right chain segments are in the topologically nontrivial phase and host Majorana bound states (MBSs) at their edges. The central region is topologically trivial. Stars denote the positions of zero-energy MBSs.

in the central region: $\tilde{c}_n = c_n$ for $m_1 + 1 \leq n \leq m_2 - 1$. Then, we can diagonalize H_C in momentum space,

$$H_C = \sum_k \epsilon(k) \tilde{c}_k^\dagger \tilde{c}_k, \tag{5}$$

where $\epsilon(k) = -\mu_C - t\cos(a_0 k)$. We introduced the lattice spacing a_0, and the momentum k is in the first Brillouin zone, $k \in [-\pi/a_0, \pi/a_0]$, and is quantized in units of $2\pi/(a_0 N_\infty)$. The operators in momentum space are defined by $\tilde{c}_k = N_\infty^{-1/2} \sum_{n=1}^{N_\infty} e^{-ika_0 n} \tilde{c}_n$.

If the three segments are not coupled ($H_{LC} = H_{RC} = 0$), our choice of parameters entails that the left and right segments are gapped due to the superconducting pairing and the width of the gap is $2\Delta = 2t$. Moreover, the left chain contains at its edges the free zero-energy MBSs γ_1 and γ_{m_1}, and the right chain contains γ_{m_2} and γ_N. In terms of the electron operators, these are given by,

$$\begin{aligned}
\gamma_1 &= 2\mathrm{Im}\, c_1 = -i(c_1 - c_1^\dagger), \\
\gamma_{m_1} &= 2\mathrm{Re}\, c_{m_1} = c_{m_1} + c_{m_1}^\dagger, \\
\gamma_{m_2} &= 2\mathrm{Im}\, c_{m_2} = -i(c_{m_2} - c_{m_2}^\dagger), \\
\gamma_N &= 2\mathrm{Re}\, c_N = c_N + c_N^\dagger.
\end{aligned} \tag{6}$$

Now, we introduce tunneling between the side chains and the central chain. Because there are no terms beyond nearest-neighbor terms in Eq. (1), only the Majorana states γ_{m_1} and γ_{m_2} are coupled to the central chain [17],

$$\begin{aligned}
H_{LC} &= -\frac{t_{LC}}{2} \gamma_{m_1} (\tilde{c}_{m_1+1} - \tilde{c}_{m_1+1}^\dagger), \\
H_{RC} &= -\frac{i t_{RC}}{2} (\tilde{c}_{m_2-1} + \tilde{c}_{m_2-1}^\dagger) \gamma_{m_2}.
\end{aligned} \tag{7}$$

Note that for our choice of parameters the Dirac fermions d_n of the left and right chains are not coupled to the remaining system. Therefore, we can discard the operators $H_{L,R}$ in the following discussion and use

$$H_0 = H_C + H_{LC} + H_{RC}. \tag{8}$$

The Hamiltonian (8) can easily be solved exactly. We are particularly interested in the coupling between γ_{m_1} and γ_{m_2}, mediated by the central chain. For $\mu_C < t$, the central

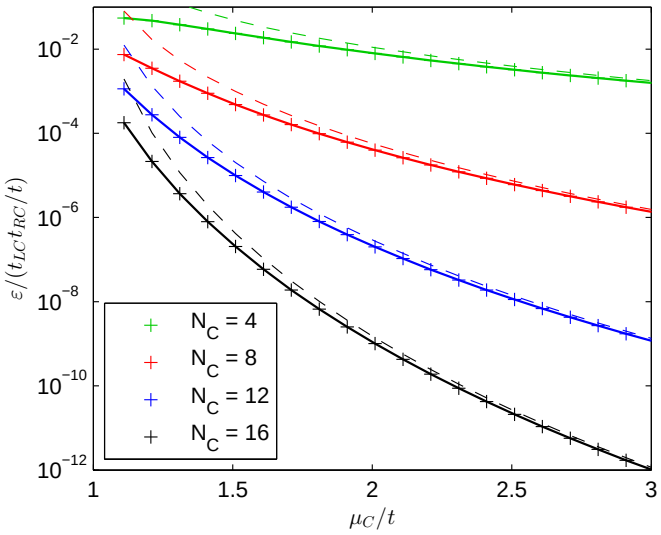

Figure 2. Splitting of the MBSs as a function of chemical potential μ_C and the number of lattice sites N_C of the central region. The crosses indicate the numerically exact solution of the inhomogeneous Kitaev chain. The solid line represents the splitting calculated numerically using periodic boundary conditions. The dashed line shows the approximation Eq. (9).

chain becomes gapless and real electrons and holes can tunnel to and from the MBS. In this regime, the overlap of the MBSs turns out to be very sensitive to system parameters, and the boundary conditions of the central region become important. The MBS self-energy acquires an imaginary part, indicating a level broadening and thus a finite lifetime of the MBS. In the continuum limit, the effect of the metallic central region thus resembles that of a fermionic bath which has been investigated in detail in Ref. [18].

On the other hand, for $\mu_C > t$, the central chain has a gap of width $2(\mu_C - t)$. The corresponding band structure (for weakly coupled chains) is shown in Fig. 1. In this regime, electron cotunneling is the only process leading to a nonzero overlap of the Majorana levels γ_{m_1} and γ_{m_2}. This overlap causes a finite level splitting of the MBS, which for $\mu_C \gg t$ becomes

$$\varepsilon = t_{LC}t_{RC}\frac{e^{-(N_C-1)\mathrm{arccosh}(\mu_C/t)}}{t\sqrt{(\mu_C/t)^2-1}}. \tag{9}$$

As expected, this splitting decays exponentially with increasing length N_C of the central region. The corresponding decay length $\xi = a_0/\mathrm{arccosh}(\mu_C/t)$ diverges as $(\mu_C/t-1)^{-1/2}$ for $\mu_C \to t$. The level splitting (9) can also be found from the exact numerical solution of the full Hamiltonian (1). A comparison between the exact numerical result and the approximation (9) is shown in Fig. 2.

In Ref. [15], we calculated the level splitting for a minimal model containing two MBS coupled via a gapped region with quadratic spectrum $\epsilon(k) = k^2/(2M) - \mu_0$. To compare the energy splitting (9) with that model, we need to take the continuum limit of the Kitaev chain by sending the lattice constant $a_0 \to 0$, while keeping the total length $L_C = N_C a_0$ constant. Let us assume that $|\mu_C| \gtrsim t$. Near the bottom of the band the spectrum of the uncoupled

central Kitaev chain is quadratic with effective mass $M = 1/(a_0^2 t)$ and chemical potential $\mu_0 = -|\mu_C| + t$. Then, one finds for small $|\mu_0| \ll t$,

$$\varepsilon \approx a_0 t_{LC} t_{RC} \frac{e^{-L_C/\xi}}{2|\mu_0|\xi} \tag{10}$$

where $\xi = (2M|\mu_0|)^{-1/2}$ is the decay length of the MBS into the gapped system.

If we focus on the gapped regime ($\mu_C > t$), we can derive a simple effective low-energy theory of the coupled Majorana modes γ_{m_1} and γ_{m_2} by integrating out the central region. This leads to an effective retarded interaction between γ_{m_1} and γ_{m_2}. In the low-energy (long-time) limit at energy scales small compared to $(\mu_C^2 - t^2)/\mu_C$, we can neglect the retardation and obtain the effective low-energy Hamiltonian

$$H_{\text{eff}} = \frac{i\varepsilon}{2} \gamma_{m_1} \gamma_{m_2}. \tag{11}$$

In Ref. [15], we pointed out the benefits of such a coupling: if the MBS (6) are used to encode a single qubit represented by the Pauli matrix σ_z, then braiding the qubits γ_1 and γ_{m_1} will allow qubit rotations $e^{i\pi\sigma_z/4}$ [12]. Braiding the MBS γ_{m_1} and γ_{m_2} corresponds to the operator $e^{i\pi\sigma_x/4}$. The set of these topologically protected operations is insufficient to reach arbitrary points on the Bloch sphere. In contrast, the Hamiltonian (11) with a tunable energy ε allows qubit rotations of the form $U_\varepsilon(t) = \exp(-i\varepsilon t \sigma_x/2)$. By combining these operations with braiding, it is possible to realize arbitrary single-qubit rotations.

In the following, we shall demonstrate that this coupling Hamiltonian can be engineered by using the interaction of the Kitaev chain with a microwave cavity field.

3. Coupling of Majorana bound states to photons

In the proposed solid-state devices [5, 6, 7], MBS exist as quasiparticles consisting of an equal-weight superposition of a particle and a hole. Therefore, they may interact with photons despite the fact that they are on average chargeless. In order to gain further insight into this coupling, we shall use the Hamiltonian of Ref. [7], and couple it to an electric field using the minimal coupling substitution $\vec{p} \to \vec{p} - e\vec{A}$, where e is the elementary charge and $\vec{A}$ is the vector potential.

The model Hamiltonian for a semiconductor nanowire along the y-axis reads

$$\begin{aligned} H_{\text{nw}} = \int dy \Bigg\{ & \sum_{\sigma=\uparrow,\downarrow} \psi_\sigma^\dagger(y) \left[-\frac{1}{2M}\frac{\partial^2}{\partial y^2} - \mu_0 - iu\sigma\frac{\partial}{\partial y} \right] \psi_\sigma(y) \\ & + \sum_{\sigma=\uparrow,\downarrow} B\psi_\sigma^\dagger(y)\psi_{-\sigma}(y) + \left[\Delta_0 \psi_\uparrow^\dagger(y)\psi_\downarrow^\dagger(y) + \text{h.c.} \right] \Bigg\}. \end{aligned} \tag{12}$$

Here, μ_0 denotes the chemical potential, and u is the strength of the Rashba spin-orbit coupling pointing in the z direction. B is a perpendicular magnetic field in the x direction. Finally, the induced s-wave pairing strength is denoted by Δ_0. It has been shown that for $B > \Delta_0$, this model exhibits MBS at the edges for $|\mu_0| < \sqrt{B^2 - \Delta_0^2}$, whereas it is in the topologically trivial phase for $|\mu_0| > \sqrt{B^2 + \Delta_0^2}$.

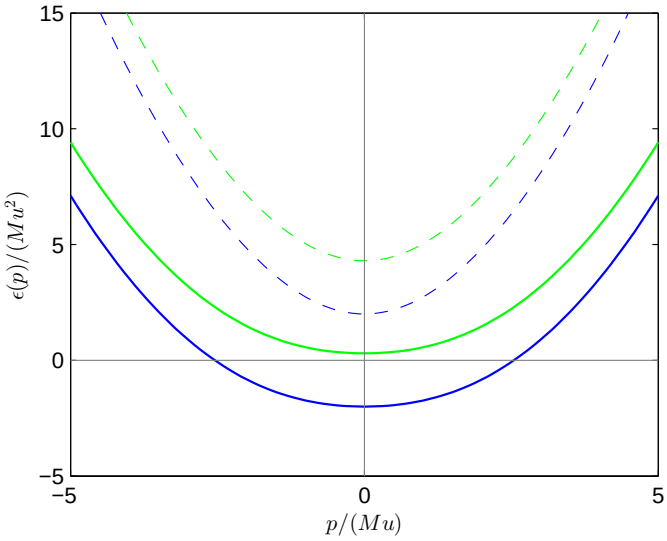

Figure 3. Single-particle spectrum corresponding to Eq. (12) for $\Delta_0 = 0$. Blue (dark grey) lines are for the topologically nontrivial phase ($\mu_0 = 0$, $B = 2Mu^2$), green (light gray) lines are for the trivial phase ($\mu_0 = -2.3Mu^2$, $B = 2Mu^2$). For the mapping onto a spinless Kitaev chain, the higher-energy parts of the spectrum (dashed lines) are neglected.

Mapping Eq. (12) on a Kitaev chain becomes most transparent in the regime $B \gg \Delta_0, Mu^2$. The band structures in the topologically trivial (nontrivial) phases are depicted in Fig. 3. In the nontrivial regime, we can choose $\mu_0 = 0$ and the band gap is proportional to the pairing potential Δ_0. In the trivial regime, on the other hand, we choose $-\mu_0 \gtrsim B$ and the band gap is $|\mu_0| - B$. One obtains a low-energy theory by retaining the lower branches $\psi_-(p)$ of both spectra. In the nontrivial region, the result is a spinless p-wave superconductor, whereas the trivial region becomes a spin-polarized electron system. Both systems may be described by Kitaev chains in the respective topological phases. For a fixed lattice spacing a_0, the parameters of the homogeneous Kitaev chain

$$H_K = -\sum_{n=1}^{N} \mu c_n^\dagger c_n - \frac{1}{2}\sum_{n=1}^{N-1} (t c_n^\dagger c_{n+1} + \Delta c_n c_{n+1} + \text{h.c.}) \tag{13}$$

are related to those of the model Hamiltonian H_{nw} as follows,

$$\mu = \mu_0 + B - \frac{1}{Ma_0^2}, \quad t = \frac{1}{Ma_0^2}, \quad \Delta = \frac{2\Delta_0 u}{Ba_0}\,. \tag{14}$$

For our proposed coupling scheme, the band gap has to be larger in the nontrivial region than in the trivial regions, so we will assume that $|\mu_0|, B \gg \Delta_0$, whereas $|\mu_0| - B \ll \Delta_0$.

The coupling to a weak vector potential $\vec{A}(\vec{r})$ in a microwave cavity can now be investigated using the minimal coupling substitution $-i\partial/\partial\vec{r} \to -i\partial/\partial\vec{r} - e\vec{A}(\vec{r})$ in the Hamiltonian (12). We assume that the cavity electric field $\vec{E} = -d\vec{A}/dt$ is oriented along the wire (y) axis, i.e., the wire axis is perpendicular to the cavity axis. Moreover, we assume that $\vec{E}(\vec{r})$ is spatially constant along the length of the wire, which is a good approximation for current experimental setups [8] and typical microwave wavelengths. In

that case, $A_y = E_{\mathrm{rms}}(a + a^\dagger)$, where E_{rms} is the root mean square of the cavity electric field, and a ($a^\dagger$) is the annihilation (creation) operator for the cavity mode. Since A_y is position-independent, it commutes with the momentum operator, so the electron-photon coupling Hamiltonian becomes

$$H_{\mathrm{el-ph}} = -\frac{ieA_y}{M}\int dy \psi_-^\dagger(y)\partial_y\psi_-(y). \tag{15}$$

We can again discretize the spatial integral. For a lattice spacing a_0, the result reads

$$H_{\mathrm{el-ph}} = \frac{eA_y}{2Ma_0}\sum_n \left(ic_n^\dagger c_{n+1} + \mathrm{h.c.}\right) \propto (a + a^\dagger)\sum_n c_n^\dagger c_{n+1} + \mathrm{h.c.} \tag{16}$$

In conclusion, an electric field gives rise to a change in the hopping matrix element between neighboring lattice sites. The expression (16) holds in both the topological trivial and nontrivial regimes. We expect the same type of coupling also at interfaces between different phases, although the coupling constant will then depend on the overlap between the wavefunctions in both regions and on their spin structure.

4. Inhomogeneous Kitaev chain in a microwave cavity

Let us assume that the inhomogeneous Kitaev chain is brought into a driven microwave cavity [14]. We consider one cavity mode with frequency Ω and assume that the cavity is driven with a frequency Ω_L,

$$H_{\mathrm{cav}}(\tau) = \Omega a^\dagger a + a\varphi e^{i\Omega_L\tau} + a^\dagger\varphi^* e^{-i\Omega_L\tau} + H_{\mathrm{cav,d}}, \tag{17}$$

where τ is the time, a is the bosonic operator of the cavity mode, φ represents amplitude and phase of the drive, and $H_{\mathrm{cav,d}}$ contains damping terms, which produce a nonzero line width κ.

We assume that the wavelength of the field $\lambda = c/\Omega$ is much longer than the Kitaev chain, so we can treat the field as constant along the Kitaev chain. The cavity field $E \propto a + a^\dagger$ acts on the electrons forming the Kitaev chain. Thus, we use the Hamiltonian (1) and supplement it by electron-photon coupling terms (16).

For the numerical solution of the system, we represent the Kitaev Hamiltonian (1) as $H_K = \frac{1}{2}A^\dagger\mathcal{H}_K A$, where $A^\dagger = (c_1^\dagger, \ldots, c_N^\dagger, c_1, \ldots, c_N)$ and $\mathcal{H}_K$ is a complex $2N \times 2N$ matrix. In the absence of coupling between the three regions, the matrix $\mathcal{H}_K$ has a fourfold degenerate eigenvalue at zero energy reflecting the four MBS (6). The corresponding basis of the zero-energy eigenspace is,

$$\begin{aligned} |\psi_1\rangle &= \frac{i}{\sqrt{2}}\left(|1\rangle - |1+N\rangle\right), \qquad |\psi_{m_1}\rangle = \frac{1}{\sqrt{2}}\left(|m_1\rangle + |m_1+N\rangle\right) \\ |\psi_N\rangle &= \frac{1}{\sqrt{2}}\left(|N\rangle + |2N\rangle\right), \qquad |\psi_{m_2}\rangle = \frac{i}{\sqrt{2}}\left(|m_2\rangle - |m_2+N\rangle\right) \end{aligned} \tag{18}$$

where $|n\rangle$ is the vector with components $|n\rangle_j = \delta_{nj}$ for $n \in \{1, \ldots, 2N\}$. For the numerical simulation, we shall assume that the system is initially prepared in the state $|\psi_{m_1}\rangle$. At time $\tau = 0$, the microwave field is switched on. The time evolution $|\psi_{m_1}(\tau)\rangle = e^{-i\mathcal{H}_K\tau}|\psi_{m_1}\rangle$ then leads to Rabi oscillations between the states $|\psi_{m_1}\rangle$ and $|\psi_{m_2}\rangle$.

To apply the proposed coupling mechanism for qubit rotations, the gap in the topologically nontrivial left and right regions should exceed the gap in the topologically trivial central region, as shown in Fig. 1. Moreover, the photon frequency Ω should be slightly below the gap in the central region, and the left and right regions much longer than the central region. This choice of parameters ensures that the two MBS in the left region (γ_1 and γ_{m_1}) and the right region (γ_{m_2} and γ_N) remain unaffected by the photon field, whereas γ_{m_1} and γ_{m_2} will be coupled. In our numerical simulations, we choose $\mu_L = \mu_R = 0$. In this case, the MBS within the left and right regions are mutually uncoupled, so it is sufficient to consider small lengths $N_{L,R}$.

4.1. Classical microwave field

Let us now first consider the case where the microwave field can be treated classically. Then, our Hamiltonian reads

$$H = H_K - \beta\sqrt{n_{\rm ph}}\cos(\Omega_L\tau)\sum_{n=1}^{N}\left(c_n^\dagger c_{n+1} + \text{h.c.}\right), \tag{19}$$

where β is the effective electron-photon coupling amplitude and $n_{\rm ph}$ is the number of photons in the cavity. Transforming the Hamiltonian into the frame rotating at the drive frequency Ω_L and performing a rotating-wave approximation, we obtain the time-independent Hamiltonian

$$\begin{aligned} H^{\rm RWA} = & -(\mu_C - \Omega_L)\sum_{n=m_1+1}^{m_2-1} c_n^\dagger c_n - \frac{t}{2}\sum_{n=m_1+1}^{m_2-2}\left(c_n^\dagger c_{n+1} + \text{h.c.}\right) \\ & - \frac{\beta\sqrt{n_{\rm ph}}}{2}\left[\gamma_{m_1}\left(c_{m_1+1} - c_{m_1+1}^\dagger\right) + i\gamma_{m_2}\left(c_{m_2+1}^\dagger + c_{m_2+1}\right)\right]. \end{aligned} \tag{20}$$

Within this approximation, the effective chemical potential of the central region is shifted to a new value $\mu_C \to \mu_C - \Omega_L$. Therefore, the effective gap of the central region can be tuned by changing the microwave frequency Ω_L. The coupling between MBS and the central region can be controlled by the drive strength which determines $n_{\rm ph}$.

In Fig. 4, we plot Rabi oscillations of the MBS γ_{m_1} as a function of time, and compare the full numerical solution of the classically driven Hamiltonian (19) to the corresponding result of Eq. (20). We find that for $t \ll \Omega_L < \mu_C$, both results are in excellent agreement. Moreover, the oscillation frequency qualitatively agrees with the approximation (9). The deviations from the exact numerical result are of the same order as the deviations shown in Fig. 2 and are mostly due to the fact that the analytical result (9) assumed $\mu_C \gg t$. The agreement between rotating wave approximation and the exact solution decreases for $\Omega_L < t$. In that case, counter-rotating terms can no longer be neglected and lead to pronounced oscillations visible in the exact solution, see Fig. 5.

4.2. Liouville equation in the quantum regime

The inhomogeneous Kitaev chain coupled to a damped photon mode can be solved numerically if we truncate the photon Hilbert space to a finite maximum photon number q_c.

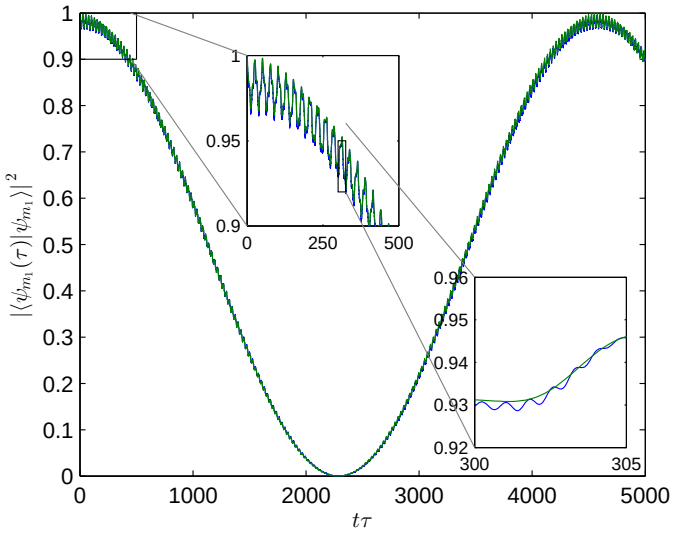

Figure 4. Comparison between rotating-wave approximation (green line), see Eq. (20), and the numerically exact classically driven time evolution (blue line), see Eq. (19). Here, τ is the time, and t the hopping amplitude. We choose parameters $\Omega_L = 3.95t$ and $\beta = 0.1t$, $N_L = N_R = 2$, $N_C = 4$, $\mu_L = \mu_R = 0$, $\mu_C = 5t$, $\Delta_L = \Delta_R = t$, $\Delta_C = 0$.

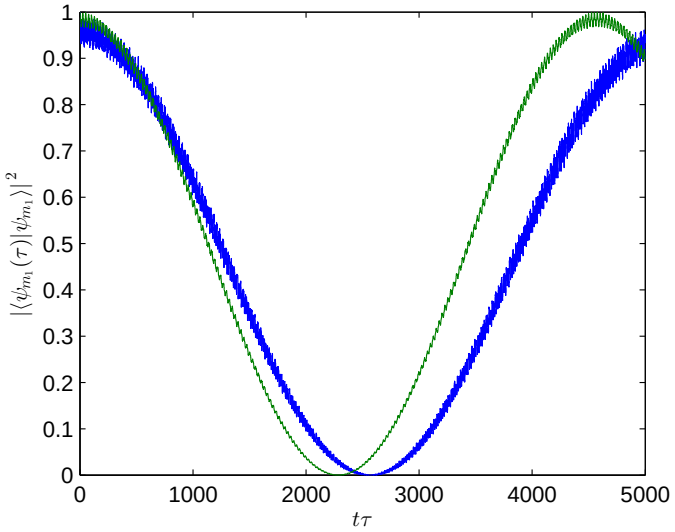

Figure 5. The rotating-wave approximation (green line) deteriorates for $\Omega_L < t$. We choose parameters $\Omega_L = 0.45t$, $\mu_C = 1.55t$. The remaining parameters are the same as in Fig. 4.

In that case, we can express the system Hamiltonian in the basis $|q, n\rangle$, where $q \in \{0, \ldots, q_c\}$ denotes the number of photons, and the single-fermion states $|n\rangle$ for $n \in \{1, \ldots, 2N\}$ were defined in Eq. (18). The Hamiltonian matrix thus has dimension $2Nq_c$. To find Rabi oscillations numerically, we solve the Liouville equation governing the time evolution of the system density matrix $\rho(\tau)$,

$$\frac{d}{d\tau}\rho(\tau) = \mathcal{L}\rho(\tau). \tag{21}$$

The Liouville superoperator $\mathcal{L}$ consists of terms describing the Kitaev chain, the photon field, the electron-photon coupling, and the damping, respectively,

$$\mathcal{L}\rho = -i[H_K, \rho] - i[H_{\rm ph}, \rho] - i[H_{\rm el,ph}, \rho] + \mathcal{L}_{\rm damping}\rho. \tag{22}$$

The Hamiltonian H_K for the Kitaev chain is given in Eq. (1). We use a constant $t_n = t$, and measure all energies relative to t. We again separate the Kitaev chain into three segments, with boundaries at $1 \leq m_1 < m_2 \leq N$, and choose the parameters in such a way that the outer segments are in the topologically nontrivial phase, whereas the central chain is topologically trivial. Within each of the segments, the parameters μ_n and Δ_n are constant.

The coherently driven cavity mode with resonance frequency Ω is described by the Hamiltonian $H_{\rm ph}$, which contains the photon operators a and $a^\dagger$, and a damping term of Lindblad form,

$$\begin{aligned} H_{\rm ph}(\tau) \quad &= \Omega a^\dagger a + a\varphi(\tau)e^{i\Omega_L\tau} + a^\dagger\varphi^*(\tau)e^{-i\Omega_L\tau}, \\ \mathcal{L}_{\rm damping}\rho &= \frac{\kappa}{2}(2a\rho a^\dagger - a^\dagger a\rho - \rho a^\dagger a). \end{aligned} \tag{23}$$

Here, $\varphi(\tau)$ encodes the (slowly varying) amplitude and phase of the external drive, Ω_L is the drive frequency, and κ is the photon damping rate. Last but not least, the electron-photon coupling Hamiltonian has the form derived in Eq. (16),

$$H_{\rm el-ph} = -\frac{\beta}{2}(a + a^\dagger)\sum_{n=1}^{N-1}\left(c_n^\dagger c_{n+1} + \text{h.c.}\right) \tag{24}$$

which has been used before in Ref. [14]. We solve the Liouville equation by representing the density matrix as a vector with $(2Nq_c)^2$ components, and the Liouville superoperator as a $(2Nq_c)^2 \times (2Nq_c)^2$ matrix acting on this vector. The number of matrix entries scales with the fourth power of the Hilbert space dimension, but the matrix is sparse and thus remains amenable to a numerical solution.

We proceed to solve the Liouville equation in real time using a fourth-order Runge-Kutta solver. We start with an initial fermionic state $|\psi_{m_1}\rangle$, and assume that the initial state contains one photon. Therefore, according to Eq. (18), the full system state is $|\psi_i\rangle = \frac{1}{\sqrt{2}}\left(|1, m_1\rangle + |1, m_1 + N\rangle\right)$ and the initial density matrix corresponds to the pure state $\rho_i = |\psi_i\rangle\langle\psi_i|$. To observe Rabi oscillations of MBS, we plot in Fig. 6 the time-dependent fidelities of the two fermionic states

$$\mathcal{F}_{m_{1,2}}(\tau) = \text{Tr}\left[\rho(\tau)\left(\mathbb{I}_{\rm ph} \otimes \left|\psi_{m_{1,2}}\right\rangle\left\langle\psi_{m_{1,2}}\right|\right)\right], \tag{25}$$

where $\mathbb{I}_{\rm ph}$ denotes the identity operator in the photon system. The solution of the Liouville equation reveals damped Rabi oscillations with a damping rate proportional to κ. For weak damping, the oscillation frequency agrees qualitatively with the results for classical driving in Sec. 4.1.

5. Conclusions

In conclusion, we have studied an inhomogeneous Kitaev chain consisting of two topologically nontrivial regions separated by a trivial, gapped region. Integrating out the

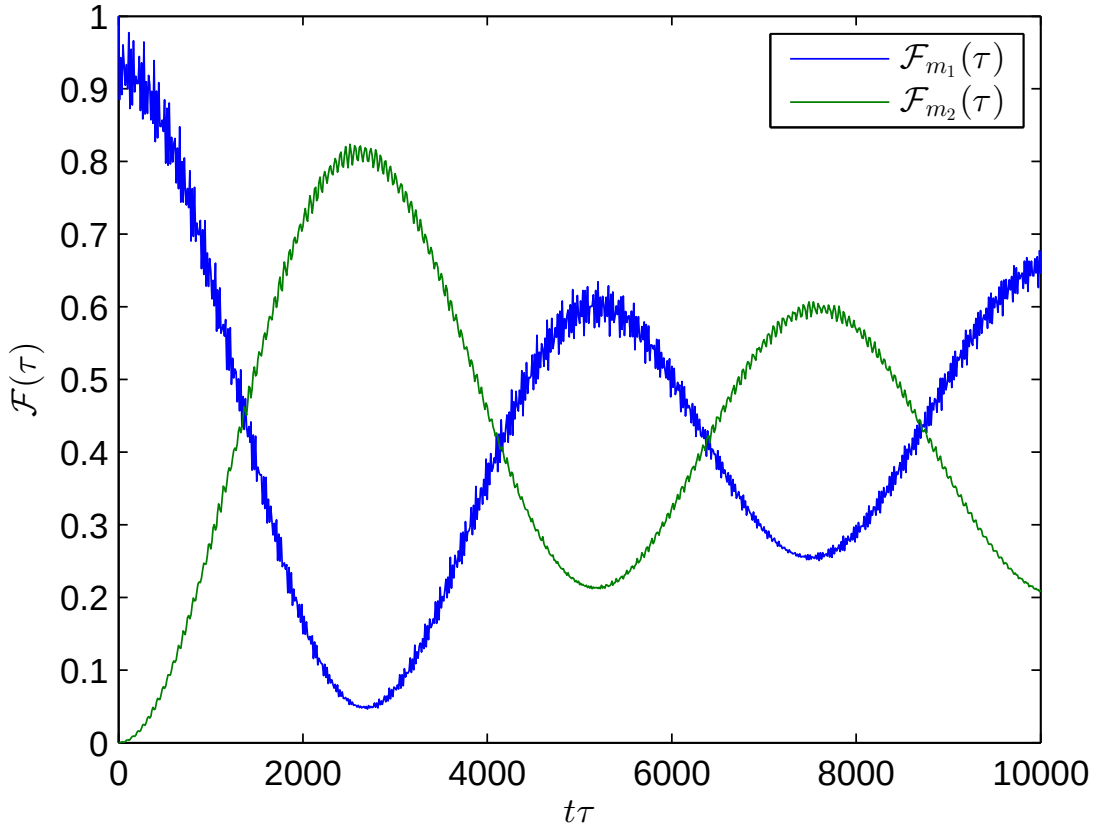

Figure 6. Damped Rabi oscillations of the Majorana bound state for a strongly damped quantized photon field ($\kappa = 2 \times 10^{-4}t$). The solution was determined from the Liouville equation (21). Parameters: $\Omega = 0.45t$, $\beta = 0.1t$, $N_L = N_R = 2$, $N_C = 4$, $\mu_L = \mu_R = 0$, $\mu_C = 1.5t$, $\Delta_L = \Delta_R = t$, $\Delta_C = 0$.

central gapped region leads to an effective coupling between the two Majorana bound states at the interface between the left region (right region) and the central region. The coupling constant decays exponentially with the length of the central region; the decay length depends on the chemical potential of the central region and diverges if the gap closes. Embedding the chain into a microwave cavity makes this decay length tunable. If the microwave frequency approaches the band gap of the topologically trivial region, the coupling between Majorana bound states adjacent to the central region can be exponentially enhanced. Since this coupling is controllable, it can be used to implement rotations of a qubit encoded in Majorana bound states. The qubit rotations achievable using this coupling, combined with braiding operations, are general enough to allow arbitrary single-qubit gates.

References

[1] Kitaev A Y 2001 *Physics-Uspekhi* **44** 131
[2] Beenakker C W J 2011 ArXiv:1112.1950
[3] Leijnse M and Flensberg K 2012 *Semiconductor Science and Technology* **27** 124003

[4] Alicea J 2012 *Rep. Prog. Phys.* **75** 076501
[5] Sato M and Fujimoto S 2009 *Phys. Rev. B* **79** 094504
[6] Lutchyn R M, Sau J D and Das Sarma S 2010 *Phys. Rev. Lett.* **105** 077001
[7] Oreg Y, Refael G and von Oppen F 2010 *Phys. Rev. Lett.* **105** 177002
[8] Mourik V, Zuo K, Frolov S M, Plissard S R, Bakkers E P A M and Kouwenhoven L P 2012 *Science* **336** 1003
[9] Rokhinson L P, Liu X and Furdyna J K 2012 *Nat. Phys.* **8** 795
[10] Deng M T, Yu C L, Huang G Y, Larsson M, Caroff P and Xu H Q 2012 ArXiv:1204.4130v1
[11] Das A, Ronen Y, Most Y, Oreg Y, Heiblum M and Shtrikman H 2012 ArXiv:1205.7073v2
[12] Nayak C, Simon S H, Stern A, Freedman M and Das Sarma S 2008 *Rev. Mod. Phys.* **80** 1083
[13] Schoelkopf R J and Girvin S M 2008 *Nature* **451** 664
[14] Trif M and Tserkovnyak Y 2012 ArXiv:1202.2649v1
[15] Schmidt T L, Nunnenkamp A and Bruder C 2012 ArXiv:1211.2201
[16] Alicea J, Oreg Y, Refael G, von Oppen F and Fisher M P A 2011 *Nat. Phys.* **7** 412
[17] Bolech C J and Demler E 2007 *Phys. Rev. Lett.* **98** 237002
[18] Budich J C, Walter S and Trauzettel B 2012 *Phys. Rev. B* **85** 121405